Antagonistic Peptide Technology for Functional Dissection of *CLV3/ESR* Genes in Arabidopsis[1][C][W][OA]

Xiu-Fen Song, Peng Guo, Shi-Chao Ren, Ting-Ting Xu, and Chun-Ming Liu*

Key Laboratory of Plant Molecular Physiology, Institute of Botany, Chinese Academy of Sciences, Beijing 100093, China (X.-F.S., P.G., S.-C.R., T.-T.X., C.-M.L.); and Graduate University of Chinese Academy of Sciences, Beijing 100049, China (P.G., S.-C.R., T.-T.X.)

In recent years, peptide hormones have been recognized as important signal molecules in plants. Genetic characterization of such peptides is challenging since they are usually encoded by small genes. As a proof of concept, we used the well-characterized stem cell-restricting CLAVATA3 (CLV3) to develop an antagonistic peptide technology by transformations of wild-type Arabidopsis (*Arabidopsis thaliana*) with constructs carrying the full-length *CLV3* with every residue in the peptide-coding region replaced, one at a time, by alanine. Analyses of transgenic plants allowed us to identify one line exhibiting a dominant-negative *clv3*-like phenotype, with enlarged shoot apical meristems and increased numbers of floral organs. We then performed second dimensional amino acid substitutions to replace the glycine residue individually with the other 18 possible proteinaceous amino acids. Examination of transgenic plants showed that a glycine-to-threonine substitution gave the strongest antagonistic effect in the wild type, in which over 70% of transgenic lines showed the *clv3*-like phenotype. Among these substitutions, a negative correlation was observed between the antagonistic effects in the wild type and the complementation efficiencies in *clv3*. We also demonstrated that such an antagonistic peptide technology is applicable to other *CLV3/EMBRYO SURROUNDING REGION* (*CLE*) genes, *CLE8* and *CLE22*, as well as in vitro treatments. We believe this technology provides a powerful tool for functional dissection of widely occurring *CLE* genes in plants.

In animals, small peptides are important signal molecules in neural and endocrinal systems (Feld and Hirschberg, 1996; Edlund and Jessell, 1999). In recent years, over a dozen different types of peptide hormones have been identified in plants, regulating both developmental and adaptive responses, usually through interacting with Leu-rich repeat receptor kinases localized in plasma membranes of neighboring cells (Boller and Felix, 2009; De Smet et al., 2009; Katsir et al., 2011). These peptides are often produced from genes with small open reading frames, after posttranslational processing (Matsubayashi, 2011). In addition, peptide hormones, such as CLAVATA3/EMBRYO SURROUNDING REGION (CLV3/ESR [CLE]), systemin, PHYTOSULFOKINE, AtPEP1, and EPIDERMAL PATTERNING FACTOR1 (EPF1), often have paralogs in genomes (Cock and McCormick, 2001; Yang et al., 2001; Pearce and Ryan, 2003; Huffaker et al., 2007; Hara et al., 2007). Bioinformatics analyses revealed that the Arabidopsis (*Arabidopsis thaliana*) genome contains 33,809 small open reading frames (Lease and Walker, 2006).

CLV3 acts as a secreted 12- or 13-amino acid glycosylated peptide (Kondo et al., 2006; Ohyama et al., 2009) to restrict the number of stem cells in shoot apical meristems (SAMs), through a CLV1-CLV2-SOL2 (for SUPPRESSOR OF LLP1 2, also called CORYNE)-RECEPTOR-LIKE PROTEIN KINASE2 (RPK2) receptor kinase-mediated pathway (Clark et al., 1993; Jeong et al., 1999; Miwa et al., 2008; Müller et al., 2008; Kinoshita et al., 2010; Zhu et al., 2010). All CLE family members, of which there are 83 in Arabidopsis and 89 in rice (*Oryza sativa*), carry a putative signal peptide and share a conserved 12-amino acid core CLE motif (Oelkers et al., 2008). Overexpression of *CLE* genes often shows a common dwarf and short-root phenotype (Strabala et al., 2006; Jun et al., 2010), which may not reflect their endogenous functions. Due to redundancies and difficulties in identifying mutants of these small genes, studies of CLE members are challenging. Only a few *CLE* genes have been genetically characterized, in particular, *CLV3*, *CLE8*, *CLE40*, and *CLE41* in Arabidopsis and *FLORAL ORGAN NUMBER4* (*FON4*), *FON2-LIKE CLE PROTEIN1* (*FCP1*), and *FON2 SPARE1* in rice (Fletcher et al., 1999; Hobe et al., 2003; Chu et al., 2006; Suzaki et al., 2008, 2009; Etchells and Turner, 2010; Fiume and Fletcher, 2012), while functions of other CLE members remain unknown.

As a proof of concept, we used the well-characterized *CLV3* gene to develop an antagonistic peptide technology

[1] This work was supported by the Ministry of Science and Technology of China (SQ2012CC057223), the National Natural Science Foundation of China (31121065), and the Chinese Academy of Sciences (20090491019).

* Corresponding author; e-mail cmliu@ibcas.ac.cn.

The author responsible for distribution of materials integral to the findings presented in this article in accordance with the policy described in the Instructions for Authors (www.plantphysiol.org) is: Chun-Ming Liu (cmliu@ibcas.ac.cn).

[C] Some figures in this article are displayed in color online but in black and white in the print edition.

[W] The online version of this article contains Web-only data.

[OA] Open Access articles can be viewed online without a subscription.

www.plantphysiol.org/cgi/doi/10.1104/pp.112.211029

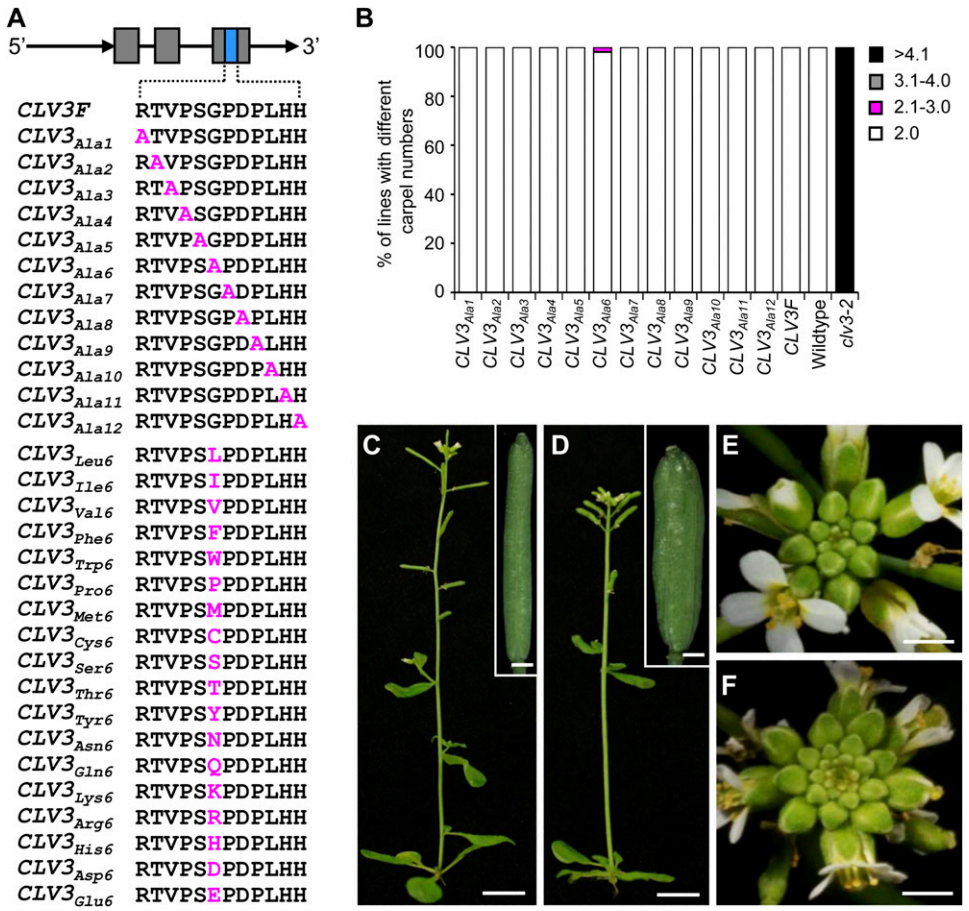

Figure 1. Amino acid-substituted *CLV3* constructs and transgenic analyses in the wild type. A, Constructs made for two-dimensional substitutions of *CLV3*. A full-length *CLV3* genomic sequence (*CLV3F*) including endogenous regulatory elements was used as the template for first dimensional Ala substitutions in the 12-amino acid peptide-coding region of CLV3 (named $CLV3_{Ala1–12}$) and second dimensional substitutions of the Gly residue at position 6 with all other 18 possible proteinaceous amino acids. B, Effects of 12 Ala-substituted CLV3s in generating dominant-negative *clv3*-like multicarpel phenotypes in the wild type. For each Ala-substituted CLV3, at least 30 transformants were obtained. The wild-type (L*er*), *clv3-2*, and *CLV3F* transgenic plants were used as controls. C and D, Wild-type plant (C) with two-carpel siliques (inset in C) and the $CLV3_{Ala6}$ transgenic plant (D) with multicarpel siliques (inset in D). Bars = 10 mm for C and D and 0.7 mm for the insets. E and F, Inflorescences of the wild type (E) and the BC1 plant of the $CLV3_{Ala6}$ transgenic line (F). Bars = 2 mm.

for functionally dissecting CLE family members in Arabidopsis. A series of constructs carrying Ala substitutions in every amino acid residue in the core CLE motif of CLV3, expressed under the endogenous *CLV3* regulatory elements, were made and introduced to wild-type Arabidopsis by transformation. This allowed us to identify the conserved Gly residue in the middle of the CLE motif was vulnerable for generating the dominant-negative *clv3*-like phenotype. We then performed second dimensional amino acid substitutions to replace the Gly with all other 18 possible proteinaceous amino acids, one at a time, and observed that the substitution of the Gly residue by Thr generated the strongest dominant-negative *clv3*-like phenotype. Further experiments showed that this technology can potentially be applied to in vitro-synthesized peptides and for functional characterization of other CLE members.

RESULTS AND DISCUSSION

Transgenic Plants Carrying CLV3 with the Gly-to-Ala Substitution in the Core CLE Motif Showed a Dominant-Negative *clv3*-Like Phenotype

The full-length 3,932-bp *CLV3* genomic sequence including a 1,857-bp 5′-upstream sequence, a 559-bp coding region, and a 1,516-bp 3′-downstream sequence was amplified (named *CLV3F*) and cloned as previously described (Song et al., 2012). Using *CLV3F* as the template, 12 constructs (named $CLV3_{Ala1–12}$) were made via PCR-based site-directed mutagenesis to replace each of the 12 residues with Ala, one at a time, in the core CLE motif of CLV3 (Fig. 1A; Song et al., 2012), and transformed into wild-type Arabidopsis (ecotype Landsberg *erecta* [L*er*]) to obtain at least 30 independent transgenic plants for each construct. We screened these transgenic plants for the multicarpel *clv3* mutant-like phenotype. As controls, wild-type and transgenic plants carrying *CLV3F* consistently showed two-carpel siliques (Fig. 1B). Although most plants carrying $CLV3_{Ala1–12}$ showed no phenotype, we identified that one plant carrying $CLV3_{Ala6}$, with the Gly residue at the position 6 substituted by Ala, exhibited multiple carpels (three to four carpels) in siliques (Fig. 1, B–D), resembling a weak *clv3* phenotype. Sequencing of the endogenous *CLV3* locus from the transgenic plant revealed no mutations, suggesting that the observed phenotype is not likely due to contamination from a recessive *clv3* mutant.

The $CLV3_{Ala6}$ transgenic line was backcrossed to the wild type, and BC1 plants still exhibited the *clv3*-like phenotype (Fig. 1, E and F), suggesting a dominant trait. Phenotypic analyses in the T2 generation showed

that the phenotype can be stably transmitted. Transgenic plants carrying the remaining 11 constructs did not give the *clv3*-like phenotype (Fig. 1B), suggesting that the Gly residue in the CLE motif is vulnerable in creating the antagonistic effect. It is plausible that peptides produced by the $CLV3_{Ala6}$ transgene are able to compete with the endogenous CLV3 peptides antagonistically to bind the CLV1-CLV2-SOL2-RPK2 receptor kinases and then block downstream signal transduction.

Optimization of the Antagonistic Peptide Technology through Second Dimensional Amino Acid Substitutions

Since the Gly-to-Ala substitution in CLV3 generated only a mild antagonistic effect in the wild type (Fig. 1B), we performed second dimensional amino acid substitutions by replacing the Gly residue, one at a time, with all other 18 possible proteinaceous amino acids through site-directed mutagenesis (Fig. 1A). All constructs, $CLV3_{Leu6}$, $CLV3_{Ile6}$, $CLV3_{Val6}$, $CLV3_{Phe6}$, $CLV3_{Trp6}$, $CLV3_{Pro6}$, $CLV3_{Met6}$, $CLV3_{Cys6}$, $CLV3_{Ser6}$, $CLV3_{Thr6}$, $CLV3_{Tyr6}$, $CLV3_{Asn6}$, $CLV3_{Gln6}$, $CLV3_{Lys6}$, $CLV3_{Arg6}$, $CLV3_{His6}$, $CLV3_{Asp6}$, and $CLV3_{Glu6}$, were transformed into wild-type Arabidopsis (L*er*), and at least 30 independent transformants were obtained for each construct. For each T1 transgenic plant, 15 siliques (five from the bottom, five from the middle, and five from the top of the inflorescence) were excised and examined under a dissection microscope for carpel numbers. Efficiencies of these constructs in creating the dominant-negative *clv3*-like phenotype are summarized in Figure 2A, based on examination of over 700 independent transgenic lines. Strikingly, all these constructs, excluding $CLV3_{Tyr6}$, were able to produce some plants with the *clv3*-like phenotype (Fig. 2A). Plants carrying $CLV3_{Thr6}$ showed the highest antagonistic effect, with approximately 70% of the $CLV3_{Thr6}$ transgenic lines exhibiting the multicarpel phenotype (Figs. 2A and 3A). Constructs of $CLV3_{Phe6}$, $CLV3_{Leu6}$, $CLV3_{Pro6}$, $CLV3_{Ile6}$, $CLV3_{Gln6}$, $CLV3_{Lys6}$, $CLV3_{Trp6}$, $CLV3_{Val6}$, and $CLV3_{Asn6}$ gave a moderate antagonistic effect, in which 35% to 60% of lines showed the *clv3*-like phenotype (Fig. 2A). The other seven constructs, including $CLV3_{Ser6}$, $CLV3_{Met6}$, $CLV3_{Arg6}$, $CLV3_{Cys6}$, $CLV3_{His6}$, $CLV3_{Asp6}$, and $CLV3_{Glu6}$, gave only a weak antagonistic effect (Fig. 2A). Transformation of $CLV3_{Tyr6}$ led to no antagonistic effect, and all 102 $CLV3_{Tyr6}$ transgenic lines examined resembled wild-type plants. Results from phenotypic analyses in 43 individual transgenic plants carrying $CLV3_{Thr6}$ are shown in Figure 3A. The carpel numbers per silique varied from two to seven among different transgenic lines (Fig. 3, A and B). No two-carpel siliques were observed in some lines, such as numbers 8, 11, 21, and 38, suggesting that there was a very strong antagonistic effect (Fig. 3A). Further analyses revealed increased numbers of flower buds in inflorescences (Fig. 3C), and enlarged SAMs in seedlings (Fig. 3D), which

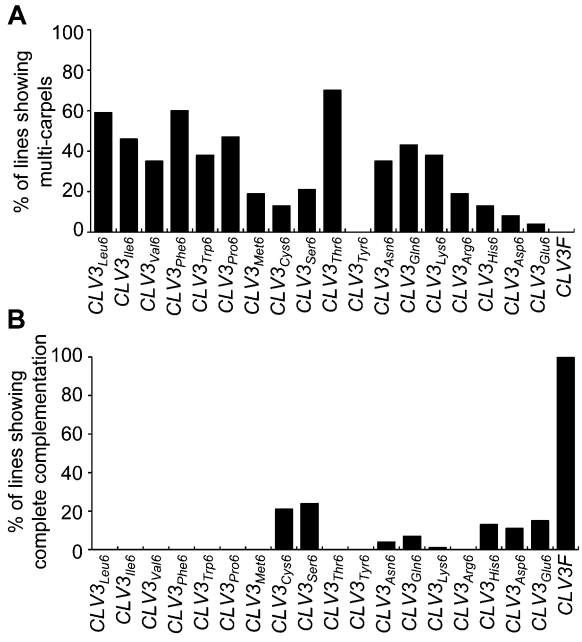

Figure 2. Antagonistic effects and complementation efficiencies of second dimensional amino acid-substituted constructs. A, Effects of 18 second dimensional amino acid-substituted CLV3 in generating the multicarpel *clv3*-like phenotype in the wild type. B, Effects of second dimensional amino acid-substituted CLV3 in complementing *clv3-2* mutants. For each amino acid-substituted CLV3, at least 30 independent transformants were obtained. *CLV3F* was used as a control.

resemble the *clv3* phenotype (Fig. 3, C and D). By comparison to constructs that gave high percentages of plants with the *clv3*-like phenotype, we noticed that substitutions of the Gly residue with other nonpolar amino acids carrying a longer side chain, such as Leu, Ile, Val, Phe, Tyr, and Pro, were more likely to generate the antagonistic effect (Fig. 2A). Interaction analyses between these antagonistic peptides and CLV1, CLV2, SOL2, and RPK2 receptor proteins may help to further understand the observed antagonistic effect.

To elucidate if the $CLV3_{Thr6}$ transgene indeed interferes with stem cell maintenance in SAMs, we crossed the $CLV3_{Thr6}$ transgenic plant with the stem cell reporter line *pCLV3::GUS* (Lenhard et al., 2002) and examined the *GUS* expression in the F2 generation. We observed a prolonged *CLV3* expression in floral buds (Fig. 4A) and an enlarged *CLV3* expression domain in SAMs (Fig. 4B), as in *clv3-2* (Fig. 4), indicating that stem cell maintenance in these $CLV3_{Thr6}$ transgenic plants was indeed disturbed. This result confirmed that the phenotype produced by the $CLV3_{Thr6}$ transgene in wild-type background is similar to the phenotype of *clv3*.

To exclude the possibility that the *clv3*-like phenotype of $CLV3_{Thr6}$ transgenic plants resulted from cosuppression of *CLV3*, we examined the expression of endogenous *CLV3* in $CLV3_{Thr6}$ transgenic plants with real-time quantitative PCR. Shoot apices were dissected

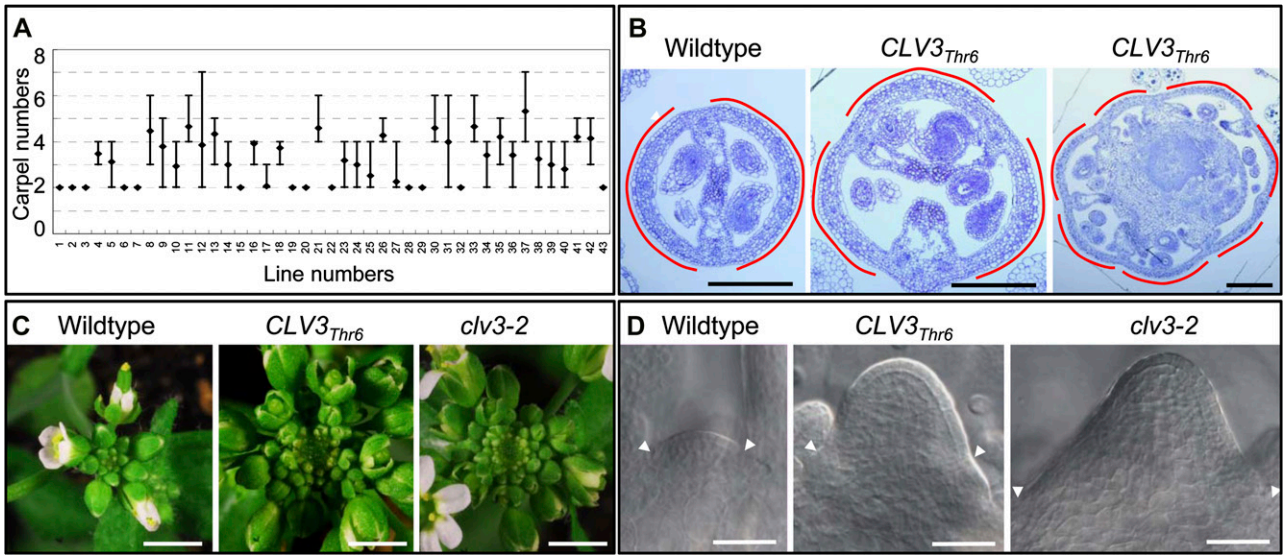

Figure 3. Effects of $CLV3_{Thr6}$ in generating the *clv3*-like phenotype. A, Among 43 individual plants transformed with $CLV3_{Thr6}$ examined, 30 showed a multicarpel *clv3*-like phenotype. Note that wild-type Arabidopsis has two carpels in siliques, and the antagonistic effect was observed in transgenic lines with more than two carpels. The diamond indicates the average carpel number, while the top and bottom bars represent the most and least carpel numbers, respectively. B, Transverse sections through siliques from $CLV3_{Thr6}$ transgenic plants with three (middle) and seven (right) carpels compared with the wild type (left) with two carpels. The red curves indicate the carpels. Bars = 200 μm. C, Inflorescences of wild-type, $CLV3_{Thr6}$ transgenic, and *clv3-2* plants. Compared with the wild type (left), inflorescences in $CLV3_{Thr6}$ transgenic plants (middle) had supernumerary flowers, as observed in *clv3-2* mutants (right). Bars = 3 mm. D, A DIC image showing the enlarged SAM in the $CLV3_{Thr6}$ transgenic plant (middle) compared with those from the wild type (left) and *clv3-2* (right). Arrowheads indicate the margins of SAMs. Bars = 50 μm.

from seedlings of wild-type (L*er*) and $CLV3_{Thr6}$ transgenic plants in parallel for RNA extraction. Real-time quantitative PCRs were performed using the same forward primer and two reverse primers in which two 3′ terminal nucleotides were unique to discriminate between the endogenous *CLV3* and the $CLV3_{Thr6}$ transgene. No significant reduction of endogenous *CLV3* expression was observed in $CLV3_{Thr6}$ transgenic plants when compared with that in L*er* wild type (P = 0.182; Supplemental Fig. S1), suggesting that there is no cosuppression occurring. Notably, the expression level of the $CLV3_{Thr6}$ transgene was higher than that of

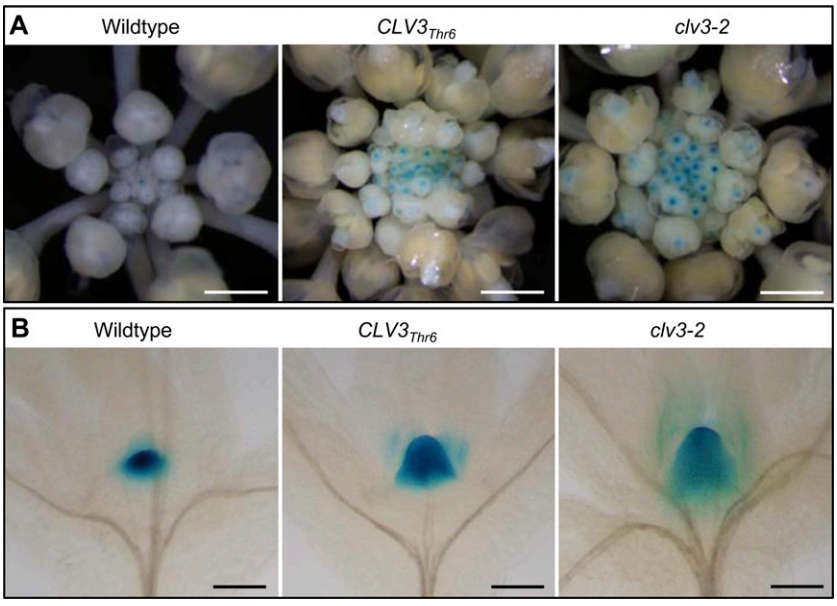

Figure 4. *GUS* expression in inflorescences and SAMs of the wild-type, $CLV3_{Thr6}$ transgenic, and *clv3-2* plants carrying *pCLV3*::*GUS*. A, *GUS* expression in inflorescences. Compared with the wild type (left), extended *GUS* expression were observed in flower buds of $CLV3_{Thr6}$ transgenic plants (center), as in *clv3-2* (right). Pictures were taken under a dissection microscope. Bars = 3 mm. B, *GUS* expression in SAMs. Compared with the wild type (left), the *GUS* expression domain was significantly enlarged in the SAM of $CLV3_{Thr6}$ transgenic plants (center), similar to *clv3-2* (right). Pictures were taken under a DIC microscope after clearing. Bars = 150 μm.

endogenous *CLV3* in the transgenic line (Supplemental Fig. S1).

Complementation Efficiencies of Second Dimensional Substitution Constructs in *clv3-2*

To characterize the relationship between antagonistic effects in the wild type and complementation efficiencies in *clv3-2*, we transformed the second dimensional substitution constructs described above into *clv3-2* mutants and analyzed their complementation efficiencies. The results showed that approximately 20% to 30% of T1 transgenic plants carrying $CLV3_{Ser6}$ or$CLV3_{Cys6}$ (Fig. 2B), and 10% to 20% of lines carrying $CLV3_{His6}$, $CLV3_{Asp6}$, or $CLV3_{Glu6}$ exhibited complete complementation, producing plants with two-carpel siliques (Fig. 2B). Less than 10% of transgenic lines carrying $CLV3_{Gln6}$, $CLV3_{Asn6}$, or $CLV3_{His6}$ showed complete complementation (Fig. 2B). No complementation was observed in transgenic *clv3-2* plants carrying $CLV3_{Leu6}$, $CLV3_{Ile6}$, $CLV3_{Val6}$, $CLV3_{Phe6}$, $CLV3_{Trp6}$, $CLV3_{Pro6}$, $CLV3_{Met6}$, $CLV3_{Thr6}$, $CLV3_{Tyr6}$, or $CLV3_{Arg6}$ (Fig. 2B), suggesting that these substitutions disrupted the function of *CLV3* completely.

A somewhat negative correlation was observed between the efficiencies of the antagonistic effect in the wild-type (Fig. 2A) and the complementation effect in *clv3-2* (Fig. 2B) in the second dimensional substitution constructs. In particular, the $CLV3_{Thr6}$ construct produced the strongest antagonistic effect in the wild type but showed no complementation in *clv3-2* (Fig. 2, A and B), whereas $CLV3_{Glu6}$ showed the weakest antagonistic effect in the wild type but a relatively high complementation efficiency in *clv3-2* (Fig. 2, A and B). This negative correlation would be expected if peptides produced by constructs with dominant-negative effect bind more strongly with the CLV3 receptors than the endogenous one but fail to execute signal transduction, thereby producing the observed antagonistic effect. For the same reason, such a construct should have a reduced complementation capacity in *clv3-2*. The $CLV3_{Tyr6}$ construct was an exception to this observed trend, as neither an antagonistic nor a complementation effect was observed (Fig. 2, A and B). It is possible that the $CLV3_{Tyr6}$ peptide produced with the Gly-to-Tyr substitution lost both of the activities of interacting with CLV3 receptors and executing downstream signal transduction.

The reason that the substitutions of the Gly residue with other amino acids gave rise to the antagonistic effect in the wild type remains to be elucidated. Studies in mouse have shown that substitution of the most critical residue in the immunogenic Hb(64-76) peptide resulted in a complete loss of downstream responses in T cells, while substitutions of two secondarily important residues created antagonistic effects (Evavold et al., 1993). Our previous in vivo complementation experiments for Ala-substituted CLV3 (Song et al., 2012) have ranked this Gly residue as the third most important one for complementing *clv3-2* among the 12 residues in the core CLE motif. Substitution of the Gly with other nonpolar amino acids with a longer side chain would restrict the rotation of the peptide produced, which may in turn lead to stronger receptor binding. It is plausible that the Gly-to-Thr substitution in CLV3 led to a nonfunctional yet strong receptor-binding peptide, preventing downstream signal transduction, and thereby generating the antagonistic effect.

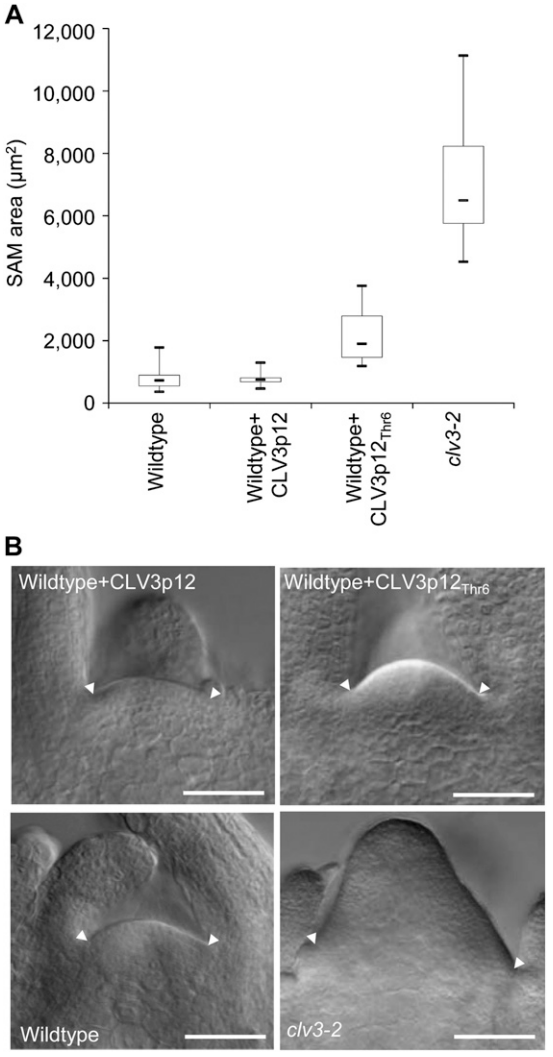

Figure 5. Enlarged SAMs observed in wild-type seedlings treated with synthetic $CLV3p12_{Thr6}$ peptides in vitro. A, Box plots of the areas of SAMs in wild-type seedlings treated with CLV3p12, or $CLV3p12_{Thr6}$ peptides, compared with those in the wild-type and *clv3-2* seedlings. Areas of SAMs were measured with ImageJ software after pictures of median sections were taken under a DIC microscope. B, DIC images of shoot apices from wild-type seedlings treated with CLV3p12 (top left) or $CLV3p12_{Thr6}$ (top right) for 9 d compared with untreated ones in the wild type (bottom left) and *clv3-2* (bottom right). Arrowheads indicate margins of SAMs. Bars = 50 μm.

The Antagonistic Effect in Vitro

It has been reported previously that synthetic 12- to 14-amino acid peptides corresponding to the CLE motif of CLV3 are functional in vitro in complementing *clv3-2* (Fiers et al., 2005; Kondo et al., 2006; Ohyama et al., 2009). To investigate if the antagonistic effect also occurs in vitro, synthetic 12-amino acid CLV3 peptides with the same Gly residue replaced by Thr (named CLV3p12$_{Thr6}$) were applied to L*er* wild-type seedlings in a liquid culture at a concentration of 10 μM, as previously described (Song et al., 2012). To prevent the potential degradation of the applied peptides, media with fresh peptides was replaced every day during the 9-d treatment. Under a differential interference contrast (DIC) microscope, enlarged SAMs were observed in CLV3p12$_{Thr6}$-treated seedlings, while no enlargements were observed in the control samples incubated in media without peptide (Fig. 5, A and B). A slight reduction of SAM size was observed in seedlings treated with normal CLV3 peptides (named CLV3p12), as reported previously (Kinoshita et al., 2007; Fig. 5, A and B).This result confirmed the presence of the antagonistic effect of the CLV3p12$_{Thr6}$ peptide in vitro. We noticed that the sizes of SAMs in CLV3p12$_{Thr6}$-treated seedlings were much smaller than those in transgenic plants carrying *CLV3$_{Thr6}$* (Figs. 3D and 5B), which suggests that the peptides applied in vitro were less effective than the peptides produced in vivo by the transgene.

To clarify if the antagonistic effect resulted from competition between CLV3p12$_{Thr6}$ and CLV3p12, we applied CLV3p12 in combination with 1, 2, and 10 times the amount of CLV3p12$_{Thr6}$ to L*er* wild-type seedlings. Media with fresh peptides was replaced every day, as described above. After a 9-d treatment, shoot apices were dissected and sizes of SAMs were measured under a DIC microscope. The meristem size of 500 μm^2 was used to assign meristems with a significant reduction after peptide treatments. About 17% of meristems treated with CLV3p12 were above 500 μm^2 in size. Under the treatments with mixed CLV3p12 and CLV3p12$_{Thr6}$, significantly increased numbers of SAMs were larger than 500 μm^2 (Supplemental Fig. S2). As the concentration of CLV3p12$_{Thr6}$ increased, the percentage of lines with SAMs larger than 500 μm^2 increased accordingly (Supplemental Fig. S2). These results suggested that CLV3p12$_{Thr6}$ can compete with CLV3p12 in vitro (Supplemental Fig. S2). It is noteworthy that even when 10 times more CLV3p12$_{Thr6}$ was added to the medium, a complete loss of CLV3p12 activity was still not observed. Since the endogenous mature CLV3 peptide has both hydroxylation and glycosylation modifications that contribute to the CLV3 activity (Ohyama et al., 2009; Shinohara and Matsubayashi,

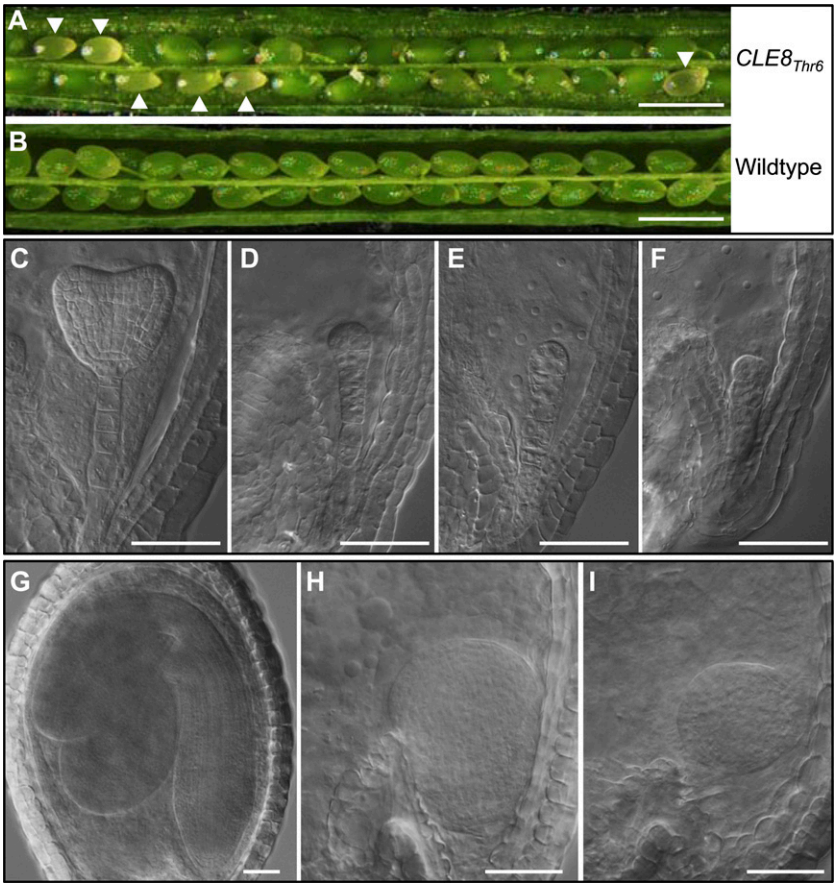

Figure 6. The embryo-lethal phenotypes in *CLE8$_{Thr6}$* transgenic plants. A and B, An opened silique of *CLE8$_{Thr6}$* transgenic plant (A) showing green wild-type ovules and transparent aborted ovules (indicated by arrowheads) compared with the wild-type silique (B) at the same stage. Bars = 1 mm. C to F, In *CLE8$_{Thr6}$* transgenic plants, both wild-type (C) and abnormal embryos (D–F) were observed in siliques 5 d after pollination. Bars = 50 μm. G to I, A wild-type cotyledonary embryo (G) and embryos with abnormal cell division pattern (H and I) in the same silique from a *CLE8$_{Thr6}$* transgenic plant. Bars = 50 μm.

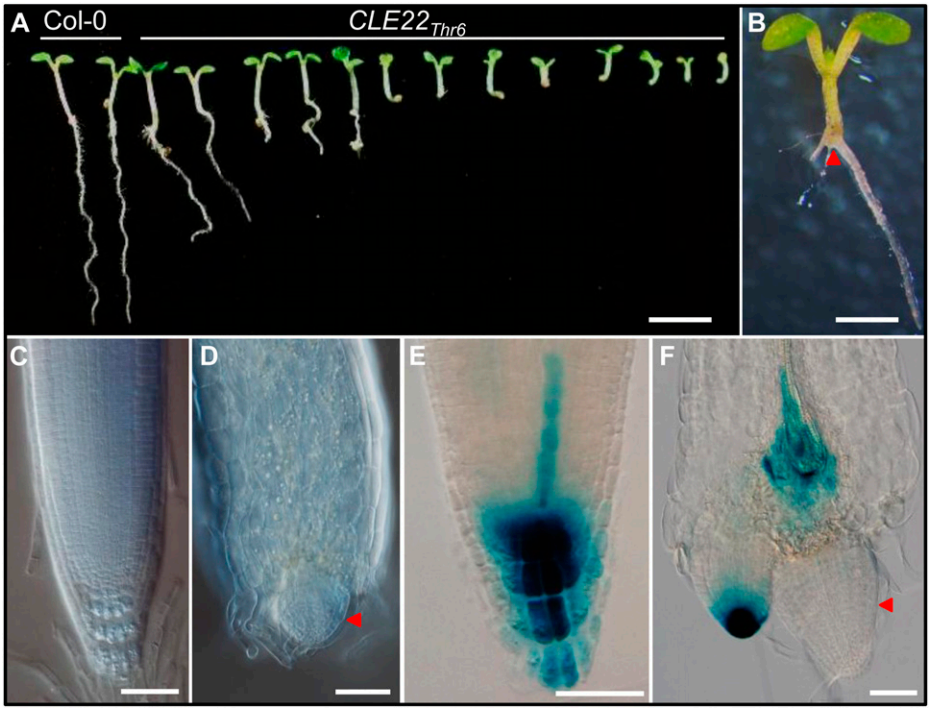

Figure 7. *CLE22*$_{Thr6}$ transgenic plants exhibited a short-root phenotype. A, Progeny of one *CLE22*$_{Thr6}$ transgenic plant, showing different degrees of the short-root phenotype. Bar = 5 mm. B, A seedling of a *CLE22*$_{Thr6}$ transgenic plant, showing termination of the primary root (arrowhead). Bar = 1 mm. C and D, Compared with the root meristems in Col-0 wild type (C), *CLE22*$_{Thr6}$ transgenic plants (D) showed the aberrant root meristem (arrowhead). Bar = 50 μm. E and F, *DR5*::*GUS* expression in root meristems in Col-0 wild-type (E) and *CLE22*$_{Thr6}$ transgenic (F) plants, showing the absence of *GUS* expression in the primary root meristem in the transgenic plant (arrowhead). Bar = 50 μm. Five-day-old seedlings were used for phenotypic observation and expression analyses.

2012), the competition observed in vitro may not entirely represent the in vivo status.

Application of the Antagonistic Peptide Technology to *CLE8*

It was reported recently that mutation or down-regulation of *CLE8* in Arabidopsis leads to defective embryo and endosperm development (Fiume and Fletcher, 2012). We used *CLE8* as an additional target to examine if the antagonistic peptide technology can be used for functional dissection of other *CLE* genes in Arabidopsis. A *CLE8*$_{Thr6}$ construct was made, with the Gly residue at the position 6 replaced by Thr, and expressed under the native *CLE8* regulatory elements including both the 5′-upstream (1,881 bp) and 3′-downstream (1,455 bp) genomic regions. We used the same Arabidopsis Columbia-0 (Col-0) ecotype as in the *cle8-1* study reported before (Fiume and Fletcher, 2012) to perform this experiment to avoid potential interference from the genetic background.

Among 78 independent *CLE8*$_{Thr6}$ T1 transgenic lines examined, eight showed embryo-lethal phenotypes (Fig. 6, A and B). The percentages of embryo-lethal seeds in these transgenic lines varied from 6% to 30% ($n > 200$ each). Phenotypes of defective embryos were similar to those reported in *cle8-1* mutants and *CLE8* down-regulated plants (Fiume and Fletcher, 2012), with abnormal cell division in the suspensor and the lower portion of the embryo at the proglobular stage (Fig. 6, C–F). When wild-type embryos reached the cotyledonary stage (Fig. 6G), some embryos in *CLE8*$_{Thr6}$ transgenic lines were arrested, with altered cell division patterns (Fig. 6, H and I). The embryo defect phenotype was also observed in the BC1 generation when the transgenic plants were pollinated reciprocally with the wild type, suggesting a dominant trait. This result suggested that the Gly-to-Thr substitution in CLE8 is able to mimic the *cle8-1* mutant phenotype, indicating that the antagonistic peptide technology can be applied to elucidate additional *CLE* genes.

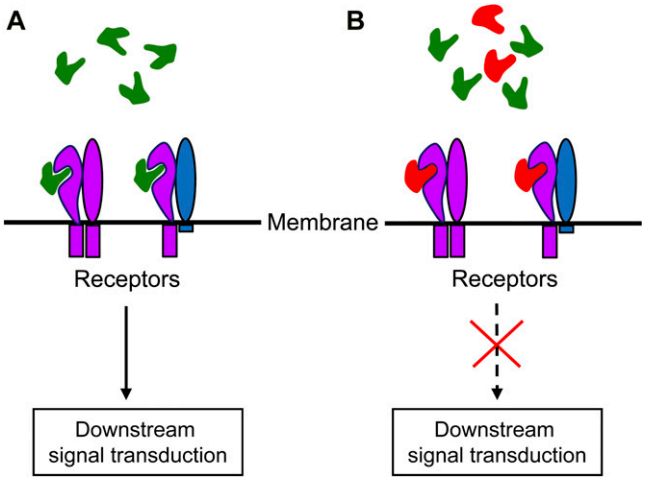

Figure 8. Schematic model of the antagonistic peptide technology. A, Endogenous CLE peptides (green) bind to its receptors, leading to downstream signal transduction. B, Peptides with the Gly-to-Thr substitution (red) bind more tightly and competitively to the receptors but fail to trigger downstream signal transduction. [See online article for color version of this figure.]

Application of the Antagonistic Peptide Technology to *CLE22*

To further verify the applicability of the technology, *CLE22* with unknown function was chosen as another target for the Gly-to-Thr substitution. A previous report has shown that *CLE22* is expressed in differentiating vascular bundles (Jun et al., 2010). The $CLE22_{Thr6}$ construct was made and transformed into the Col-0 wild-type background and expressed under the *CLE22* native promoter including 1,495-bp 5′-upstream and 1,243-bp 3′-downstream sequences. In the T2 generation, we observed that some transgenic seedlings exhibited a very short root phenotype (Fig. 7, A and B). Detailed examination revealed an almost immediate termination of the root meristem (Fig. 7, C and D). We speculated that the short-root phenotype is the consequence of arrested cell division and differentiation in roots. After crossing the $CLE22_{Thr6}$ transgenic plant with a *DR5*::*GUS* marker line (Ulmasov et al., 1997), we observed no *GUS* expression in the defective primary root meristem, suggesting the auxin maximum has disappeared. It remains to be elucidated whether the $CLE22_{Thr6}$ antagonistic effect interferes directly with the auxin flow in roots or whether it interferes with vascular differentiation first and consequently disrupts auxin flow (Fig. 7, E and F).

Among all proteinaceous amino acids, Gly is the most flexible one, which may give peptides a free rotation property. The Gly-to-Thr substitutions in the core CLE motif of CLV3, CLE8, and CLE22 may have compromised the flexibility of the peptides produced, leading to stronger interaction with corresponding receptors but disrupted downstream signal transduction, therefore creating the observed antagonistic effects (Fig. 8). Sequence alignment showed that the Gly residue located in the middle of the core CLE motif is highly conserved in the CLE family, with 90.4% identity among the 198 CLE members examined (Supplemental Fig. S3). The conserved Gly residue has also been found in several other types of peptide hormones, such as AtPEPs and EPFs in plants (Supplemental Fig. S4). Targeted expression of these genes with the Gly-to-Thr substitution may potentially help to characterize their functions.

CONCLUSION

Taken together, through two-dimensional amino acid substitutions of CLV3 and expressed under its endogenous promoters in the wild type, we identified the Gly in the peptide-coding region as the vulnerable residue in creating the antagonistic effect. Among all proteinaceous amino acids tested, substitution of the Gly residue by Thr in CLV3 gave the strongest dominant *clv3* mutant-like phenotype. We further showed that the antagonistic peptide technology is effective in generating dominant-negative phenotype in CLE8 and CLE22. We believe that the technology provides a powerful tool for the functional dissection of CLEs in plants and may potentially be used in the study of other peptide hormones.

MATERIALS AND METHODS

Plant Materials and Growth Conditions

Wild-type Arabidopsis (*Arabidopsis thaliana*) ecotype L*er* was used for all experiments except as otherwise noted. Seeds of L*er* and *clv3-2* (in L*er* background) were surface sterilized for 2 h in a desiccator with chlorine gas, as previously reported (Fiers et al., 2005), and plated on one-half-strength Murashige and Skoog basal salt medium containing 1% Suc, 0.05% MES, and 1% agar (pH 5.8). After a 2-d vernalization at 4°C, plates were cultured in a growth room with 16 h light per day at 21°C ± 1°C. After a 5-d culture, seedlings were transferred to pots filled with 1:1 mixed soil and vermiculite and grown under the same temperature and light regime. Transformation was performed via an *Agrobacterium tumefaciens*-mediated floral dip method (Clough and Bent, 1998). Transgenic plants were obtained under the selection of 25 mg L^{-1} glufosinate ammonium (Sigma-Aldrich).

Molecular Cloning

A *CLV3* genomic sequence (3,932 bp) containing 5′- and 3′-regulatory elements was cloned into a *pDONR221* vector (Life Technologies) and then subcloned into a *pBGWFS7* binary vector (Karimi et al., 2002) to produce the *CLV3F* construct. Ala-substituted *CLV3* constructs, $CLV3_{Ala1}$, $CLV3_{Ala2}$, $CLV3_{Ala3}$, $CLV3_{Ala4}$, $CLV3_{Ala5}$, $CLV3_{Ala6}$, $CLV3_{Ala7}$, $CLV3_{Ala8}$, $CLV3_{Ala9}$, $CLV3_{Ala10}$, $CLV3_{Ala11}$, and $CLV3_{Ala12}$, were made as described previously (Song et al., 2012). For the second dimensional substitutions, the Gly residue at position 6 of the core CLE motif of CLV3 was replaced by all 18 possible proteinaceous amino acids, one at a time, with a PCR-based site-directed mutagenesis kit (Transgen) to produce the constructs $CLV3_{Leu6}$, $CLV3_{Ile6}$, $CLV3_{Val6}$, $CLV3_{Phe6}$, $CLV3_{Trp6}$, $CLV3_{Pro6}$, $CLV3_{Met6}$, $CLV3_{Cys6}$, $CLV3_{Ser6}$, $CLV3_{Thr6}$, $CLV3_{Tyr6}$, $CLV3_{Asn6}$, $CLV3_{Gln6}$, $CLV3_{Lys6}$, $CLV3_{Arg6}$, $CLV3_{His6}$, $CLV3_{Asp6}$, and $CLV3_{Glu6}$. Full-length 3,597-bp *CLE8* and a 3,050-bp *CLE22* genomic sequences containing 5′ and 3′ regulatory elements were cloned into the *pDONR221* vector to produce *pDONR221-CLE8F* and *pDONR221-CLE22F*, respectively. A Gly-to-Thr substitution was introduced to the CLE motif of CLE8 and CLE22 via a site-directed mutagenesis to produce the $CLE8_{Thr6}$ and $CLE22_{Thr6}$ constructs.

Tissue Clearing

Samples of shoot apices, ovules, and roots were cleared as described (Sabatini et al., 1999) and observed under a DIC microscope (Leica DM4500). SAM areas were measured with ImageJ software as reported previously (Fiers et al., 2005).

In Vitro Peptide Assay

CLV3p12 (RTVPSGPDPLHH) and $CLV3p12_{Thr6}$ (RTVPSTPDPLHH) peptides (≥90% purity) were synthesized commercially (AuGCT Biotechnology). In vitro treatments of L*er* wild-type seedlings with 10 μM CLV3p12 and $CLV3p12_{Thr6}$ peptides were performed as previously described (Song et al., 2012). For competition assays, L*er* wild-type seedlings were treated with different concentrations of $CLV3p12_{Thr6}$ combined with 10 μM CLV3p in liquid one-half-strength Murashige and Skoog media. Media with peptides were refreshed every day. After a 9-d treatment, shoot apices were excised under a dissection microscope, cleared, and observed as previously described (Sabatini et al., 1999).

GUS Assay

Seedlings and inflorescences of L*er* wild-type, *clv3-2*, and $CLV3_{Thr6}$ transgenic plants carrying *pCLV3*::*GUS* (Lenhard et al., 2002) were examined for *GUS* expression as previously described (Fiers et al., 2004). Roots of Col-0 wild-type and $CLE22_{Thr6}$ transgenic plants carrying *DR5*::*GUS* were examined for *GUS* expression as previously described (Ulmasov et al., 1997). After the dehydration with 70%, 85%, 90%, and 100% ethanol, seedlings were cleared

and observed under a DIC microscope (Sabatini et al., 1999). Inflorescences were observed under a dissection microscope directly following dehydration.

Histological Analyses

Siliques of $CLV3_{Thr6}$ transgenic plants were fixed in a modified formaldehyde-acetic acid solution (Liu et al., 1993) for 12 h and embedded in LR White (The London Resin Company) as described in the manufacturer's manual. Embedded siliques were sectioned at 2-μm thickness using a microtome (Leica EM UC7) and stained with 0.1% toluidine blue.

Real-Time Quantitative PCR

An RNA isolation kit (Tiangen) was used to extract total RNA from shoot apices excised from seedlings of L*er* wild-type and 30 to 40 $CLV3_{Thr6}$ transgenic T2 plants. Reverse transcription was performed using a FastQuant RT kit (Tiangen). Real-time quantitative PCR was performed in a Rotor-Gene 3000 Thermocycler (Corbett Research) with a SYBR Premix ExTaq II kit (Takara). The relative expression levels were normalized against *EIF4A* through the use of a modified cycle threshold method (Livak and Schmittgen, 2001). The primers used are listed in Supplemental Table S1.

Supplemental Data

The following materials are available in the online version of this article.

Supplemental Figure S1. Real-time quantitative PCR analyses of endogenous *CLV3* and $CLV3_{Thr6}$ transgene expression in the wild type and $CLV3_{Thr6}$ transgenic plants.

Supplemental Figure S2. In vitro competition assay.

Supplemental Figure S3. Alignments of the core CLE motifs in CLE family members.

Supplemental Figure S4. Alignments of the conserved motifs in AtPEP and EPF family members.

Supplemental Table S1. List of primers used.

ACKNOWLEDGMENTS

We thank Da-Li Yu and Chen Li for assistance and John Hugh Snyder for critical reading of the article.

Received November 15, 2012; accepted January 14, 2013; published January 15, 2013.

LITERATURE CITED

Boller T, Felix G (2009) A renaissance of elicitors: perception of microbe-associated molecular patterns and danger signals by pattern-recognition receptors. Annu Rev Plant Biol **60:** 379–406

Chu H, Qian Q, Liang W, Yin C, Tan H, Yao X, Yuan Z, Yang J, Huang H, Luo D, et al (2006) The *FLORAL ORGAN NUMBER4* gene encoding a putative ortholog of Arabidopsis CLAVATA3 regulates apical meristem size in rice. Plant Physiol **142:** 1039–1052

Clark SE, Running MP, Meyerowitz EM (1993) CLAVATA1, a regulator of meristem and flower development in Arabidopsis. Development **119:** 397–418

Clough SJ, Bent AF (1998) Floral dip: a simplified method for Agrobacterium-mediated transformation of *Arabidopsis thaliana*. Plant J **16:** 735–743

Cock JM, McCormick S (2001) A large family of genes that share homology with *CLAVATA3*. Plant Physiol **126:** 939–942

De Smet I, Voss U, Jürgens G, Beeckman T (2009) Receptor-like kinases shape the plant. Nat Cell Biol **11:** 1166–1173

Edlund T, Jessell TM (1999) Progression from extrinsic to intrinsic signaling in cell fate specification: a view from the nervous system. Cell **96:** 211–224

Etchells JP, Turner SR (2010) The PXY-CLE41 receptor ligand pair defines a multifunctional pathway that controls the rate and orientation of vascular cell division. Development **137:** 767–774

Evavold BD, Sloan-Lancaster J, Allen PM (1993) Tickling the TCR: selective T-cell functions stimulated by altered peptide ligands. Immunol Today **14:** 602–609

Feld S, Hirschberg R (1996) Growth hormone, the insulin-like growth factor system, and the kidney. Endocr Rev **17:** 423–480

Fiers M, Golemiec E, Xu J, van der Geest L, Heidstra R, Stiekema W, Liu CM (2005) The 14-amino acid CLV3, CLE19, and CLE40 peptides trigger consumption of the root meristem in *Arabidopsis* through a CLAVATA2-dependent pathway. Plant Cell **17:** 2542–2553

Fiers M, Hause G, Boutilier K, Casamitjana-Martinez E, Weijers D, Offringa R, van der Geest L, van Lookeren Campagne M, Liu CM (2004) Mis-expression of the *CLV3/ESR*-like gene *CLE19* in Arabidopsis leads to a consumption of root meristem. Gene **327:** 37–49

Fiume E, Fletcher JC (2012) Regulation of *Arabidopsis* embryo and endosperm development by the polypeptide signaling molecule CLE8. Plant Cell **24:** 1000–1012

Fletcher JC, Brand U, Running MP, Simon R, Meyerowitz EM (1999) Signaling of cell fate decisions by CLAVATA3 in Arabidopsis shoot meristems. Science **283:** 1911–1914

Hara K, Kajita R, Torii KU, Bergmann DC, Kakimoto T (2007) The secretory peptide gene *EPF1* enforces the stomatal one-cell-spacing rule. Genes Dev **21:** 1720–1725

Hobe M, Müller R, Grünewald M, Brand U, Simon R (2003) Loss of CLE40, a protein functionally equivalent to the stem cell restricting signal CLV3, enhances root waving in Arabidopsis. Dev Genes Evol **213:** 371–381

Huffaker A, Ryan CA (2007) Endogenous peptide defense signals in Arabidopsis differentially amplify signaling for the innate immune response. Proc Natl Acad Sci USA **104:** 10732–10736

Jeong S, Trotochaud AE, Clark SE (1999) The *Arabidopsis CLAVATA2* gene encodes a receptor-like protein required for the stability of the CLAVATA1 receptor-like kinase. Plant Cell **11:** 1925–1934

Jun JH, Fiume E, Roeder AHK, Meng L, Sharma VK, Osmont KS, Baker C, Ha CM, Meyerowitz EM, Feldman LJ, et al (2010) Comprehensive analysis of *CLE* polypeptide signaling gene expression and overexpression activity in Arabidopsis. Plant Physiol **154:** 1721–1736

Karimi M, Inzé D, Depicker A (2002) GATEWAY vectors for *Agrobacterium*-mediated plant transformation. Trends Plant Sci **7:** 193–195

Katsir L, Davies KA, Bergmann DC, Laux T (2011) Peptide signaling in plant development. Curr Biol **21:** R356–R364

Kinoshita A, Betsuyaku S, Osakabe Y, Mizuno S, Nagawa S, Stahl Y, Simon R, Yamaguchi-Shinozaki K, Fukuda H, Sawa S (2010) RPK2 is an essential receptor-like kinase that transmits the CLV3 signal in Arabidopsis. Development **137:** 3911–3920

Kinoshita A, Nakamura Y, Sasaki E, Kyozuka J, Fukuda H, Sawa S (2007) Gain-of-function phenotypes of chemically synthetic CLAVATA3/ESR-related (CLE) peptides in *Arabidopsis thaliana* and *Oryza sativa*. Plant Cell Physiol **48:** 1821–1825

Kondo T, Sawa S, Kinoshita A, Mizuno S, Kakimoto T, Fukuda H, Sakagami Y (2006) A plant peptide encoded by *CLV3* identified by in situ MALDI-TOF MS analysis. Science **313:** 845–848

Lease KA, Walker JC (2006) The Arabidopsis unannotated secreted peptide database, a resource for plant peptidomics. Plant Physiol **142:** 831–838

Lenhard M, Jürgens G, Laux T (2002) The *WUSCHEL* and *SHOOTMERISTEMLESS* genes fulfill complementary roles in Arabidopsis shoot meristem regulation. Development **129:** 3195–3206

Liu C, Xu Z, Chua NH (1993) Auxin polar transport is essential for the establishment of bilateral symmetry during early plant embryogenesis. Plant Cell **5:** 621–630

Livak KJ, Schmittgen TD (2001) Analysis of relative gene expression data using real-time quantitative PCR and the $2^{-\Delta\Delta C}{}_T$ Method. Methods **25:** 402–408

Matsubayashi Y (2011) Post-translational modifications in secreted peptide hormones in plants. Plant Cell Physiol **52:** 5–13

Miwa H, Betsuyaku S, Iwamoto K, Kinoshita A, Fukuda H, Sawa S (2008) The receptor-like kinase SOL2 mediates CLE signaling in Arabidopsis. Plant Cell Physiol **49:** 1752–1757

Müller R, Bleckmann A, Simon R (2008) The receptor kinase CORYNE of *Arabidopsis* transmits the stem cell-limiting signal CLAVATA3 independently of CLAVATA1. Plant Cell **20:** 934–946

Oelkers K, Goffard N, Weiller GF, Gresshoff PM, Mathesius U, Frickey T (2008) Bioinformatic analysis of the CLE signaling peptide family. BMC Plant Biol **8:** 1–15

Ohyama K, Shinohara H, Ogawa-Ohnishi M, Matsubayashi Y (2009) A glycopeptide regulating stem cell fate in *Arabidopsis thaliana*. Nat Chem Biol **5:** 578–580

Pearce G, Ryan CA (2003) Systemic signaling in tomato plants for defense against herbivores. Isolation and characterization of three novel defense-signaling glycopeptide hormones coded in a single precursor gene. J Biol Chem **278:** 30044–30050

Sabatini S, Beis D, Wolkenfelt H, Murfett J, Guilfoyle T, Malamy J, Benfey PN, Leyser O, Bechtold N, Weisbeek P, et al (1999) An auxin-dependent distal organizer of pattern and polarity in the Arabidopsis root. Cell **99:** 463–472

Shinohara H, Matsubayashi Y (2012) Chemical synthesis of Arabidopsis CLV3 glycopeptide reveals the impact of Hyp arabinosylation on peptide conformation and activity. Plant Cell Physiol (in press)

Song XF, Yu DL, Xu TT, Ren SC, Guo P, Liu CM (2012) Contributions of individual amino acid residues to the endogenous CLV3 function in shoot apical meristem maintenance in Arabidopsis. Mol Plant **5:** 515–523

Strabala TJ, O'donnell PJ, Smit AM, Ampomah-Dwamena C, Martin EJ, Netzler N, Nieuwenhuizen NJ, Quinn BD, Foote HCC, Hudson KR (2006) Gain-of-function phenotypes of many *CLAVATA3/ESR* genes, including four new family members, correlate with tandem variations in the conserved CLAVATA3/ESR domain. Plant Physiol **140:** 1331–1344

Suzaki T, Ohneda M, Toriba T, Yoshida A, Hirano HY (2009) *FON2 SPARE1* redundantly regulates floral meristem maintenance with *FLORAL ORGAN NUMBER2* in rice. PLoS Genet **5:** e1000693

Suzaki T, Yoshida A, Hirano HY (2008) Functional diversification of CLAVATA3-related CLE proteins in meristem maintenance in rice. Plant Cell **20:** 2049–2058

Ulmasov T, Murfett J, Hagen G, Guilfoyle TJ (1997) Aux/IAA proteins repress expression of reporter genes containing natural and highly active synthetic auxin response elements. Plant Cell **9:** 1963–1971

Yang H, Matsubayashi Y, Nakamura K, Sakagami Y (2001) Diversity of Arabidopsis genes encoding precursors for phytosulfokine, a peptide growth factor. Plant Physiol **127:** 842–851

Zhu Y, Wang Y, Li R, Song X, Wang Q, Huang S, Jin JB, Liu CM, Lin J (2010) Analysis of interactions among the CLAVATA3 receptors reveals a direct interaction between CLAVATA2 and CORYNE in Arabidopsis. Plant J **61:** 223–233